HHS Public Access

Stereotactic Ablative Radiotherapy Induces Systemic Differences in Peripheral Blood Immunophenotype Dependent on Irradiated Site

Heather M. McGee, MD, PhD[#1,2], **Megan E. Daly, MD**[#1], **Sohelia Azghadi, MD**[1], **Susan L. Stewart, PhD**[3], **Leslie Oesterich, MD**[4], **Jeffrey Schlom, PhD**[5], **Renee Donahue, PhD**[5], **Jonathan D. Schoenfeld, MD**[9,6], **Qian Chen, BS**[7], **Shyam Rao, MD, PhD**[1], **Ruben C. Fragoso, MD, PhD**[1], **Richard K. Valicenti, MD**[1], **Robert J. Canter, MD**[7], **Emmanual M. Maverakis, PhD**[7], **William J. Murphy, PhD**[7,8], **Karen Kelly, MD**[4], and **Arta M. Monjazeb, MD, PhD**[1,7]

[1]Department of Radiation Oncology, University of California Davis Comprehensive Cancer Center

[2]Department of Radiation Oncology, Icahn School of Medicine at Mount Sinai

[3]Department of Public Health Sciences, University of California Davis School of Medicine

[4]Department of Medicine, Division of Medical Oncology, University of California Davis Comprehensive Cancer Center

[5]Laboratory of Cancer Immunology and Biology, Center for Cancer Research, National Cancer Institute, National Institutes of Health

[6]Department of Radiation Oncology, Dana-Farber/Brigham and Women's Cancer Center

[7]Laboratory of Cancer Immunology, University of California, Davis School of Medicine

[8]Department of Dermatology, University of California, Davis School of Medicine

[9]Departments of Radiation Oncology, Brigham and Women's / Dana-Farber Cancer Center and Harvard Medical School

[#] These authors contributed equally to this work.

Abstract

Purpose/Objective(s): Despite strong interest in combining stereotactic ablative radiotherapy (SAR) with immunotherapy, limited data characterize the systemic immune response following

SAR. We hypothesized that the systemic immune response to SAR differs by irradiated site due to inherent differences in the microenvironment of various organs.

Materials/Methods: Patients receiving SAR to any organ underwent prospective blood banking pre- and 1–2 weeks post-SAR. Peripheral blood mononuclear cells (PBMC) and serum were isolated. PBMC were stained with fluorophore-conjugated antibodies against T and natural killer (NK) cell markers. Cells were interrogated by flow cytometry and results were analyzed using Flow Jo software. Serum cytokine and chemokine levels were measured using Luminex. We analyzed changes from pre- to posttherapy with paired t-tests or 1-way ANOVA with Bonferroni's post-test.

Results: Thirty-one patients had evaluable PBMC for flow cytometry and thirty-seven had evaluable serum samples for Luminex analysis. Total NK cells and cytotoxic (CD56^{dim} CD16$^+$) NK cells decreased (p = 0.02) and TIM3+ NK cells increased (p = 0.04) following SAR to parenchymal sites (lung and liver), but not to bone or brain. Total memory CD4+ T cells, activated (ICOS+) and CD25+ CD4+ memory T-cells, and activated CD25+ CD8+ memory T cells increased following SAR to parenchymal sites, but not bone or brain. Circulating levels of TNF-α (p = 0.04) and multiple chemokines, including RANTES (p = 0.04), decreased after SAR to parenchymal sites, but not bone or brain.

Conclusions: Our data suggest SAR to parenchymal sites induces systemic immune changes, including a decrease in total and cytotoxic NK cells, an increase in TIM-3+ NK cells, and an increase in activated memory CD4+ and CD8+ T cells. SAR to non-parenchymal sites did not induce these changes. By comparing the immune response after radiation to different organs, our data suggest SAR induces systemic immunologic changes dependent upon irradiated site.

SUMMARY

We performed a prospective study to assess the systemic immune response 1–2 weeks following stereotactic radiation (SAR) to different organs using flow cytometry for immunophenotyping and Luminex analysis. Our results suggest SAR to parenchymal sites (lung and liver) induces systemic immune changes, including a decrease in total and cytotoxic NK cells and an increase in TIM-3+ NK cells and activated memory CD4+ and CD8+ T cells. SAR to non-parenchymal sites did not induce these changes.

INTRODUCTION:

Stereotactic ablative radiotherapy (SAR), a technique for delivering ablative doses of conformal radiotherapy over 1–5 fractions, has emerged as a standard treatment option for a variety of solid tumors, both for definitive therapy of localized disease and for local control of metastatic sites.[1,2,3,4,5,6,7] Recently, there has been considerable interest in combining radiotherapy with immunotherapy in order to use radiation as an *in situ* tumor vaccine that enhances the efficacy of immunotherapy.[8,9,10,11,12] While there are many registered, actively accruing clinical trials that incorporate radiation with immune checkpoint inhibitors,[13,14] it

is unclear how to optimize radiotherapy in these trials because there is insufficient data investigating the immune response to SAR alone.

The immunomodulatory effects of radiotherapy, particularly local immune effects on the tumor microenvironment, are well-established in preclinical models,[8,15] and include induction of immunogenic cell death,[16,17] release of antigens for T cell priming,[18] improved T cell homing to tumor sites,[19] shift in the polarization of tumor associated macrophages,[19] and destruction of immunosuppressive stromal cells in the tumor microenvironment,[20] amongst others. More recent studies suggest that hypofractionated radiation schedules produce very different biologic effects than traditional conventionally fractionated radiation.[21,22,23,24] Clinical reports of distant, or "abscopal" responses in patients have described systemic immunophenotype changes, but all of these reports have been in the setting of combined radiation and immunotherapy.[25,26,27] Several small studies have investigated the immune response to SAR for early stage lung cancer,[28,29] and more recently additional studies have investigated components of the immune response after SAR for hepatocellular carcinoma,[30] pancreatic cancer[31] and breast cancer.[32] However, we know of no published studies that directly compare changes in systemic immunophenotype and cytokine signatures following SAR without systemic therapy to different irradiated sites. Investigating differences in systemic immunophenotype after SAR based on irradiated site could be critical for the rational design of future combined SAR + immunotherapy trials.

There are well-defined, inherent differences in the immune microenvironment of different organs, from the relatively immunoprivileged brain protected by the blood-brain barrier, and immunoprivileged hematopoietic stem cell niche in the bone marrow, to the immunotolerant lung and liver, which are constantly exposed to antigens.[33,34,35] As natural killer (NK) cells comprise a large portion of the immunotolerant organs such as the lung and liver, we hypothesized that radiation to these sites may cause unique changes in specific NK cell populations.[33,36] We hypothesized that the systemic immune response to SAR would differ based on irradiated site, and set out to gain a comprehensive understanding of these differences to refine future clinical trials combining radiotherapy and immunotherapy. We prospectively collected blood samples prior to SAR and 1–2 weeks post-SAR from patients undergoing SAR to lung, liver, bone, or brain to measure changes in markers of the systemic immune response, such as cytokine/chemokine signatures and immunophenotype changes in peripheral blood mononucleated cells (PBMCs).

MATERIALS & METHODS:

PATIENTS

Patients were recruited as part of an Institutional Review Board-approved blood collection protocol at XXXXX, designed to assess the systemic immune response following SAR. Patients seen in the radiation oncology clinic in consultation for SAR were recruited by study team investigators. Eligible patients were scheduled to undergo 1–5 fractions of stereotactic body radiation therapy (SBRT) or 1–10 fractions of hypofractionated conformal radiotherapy for cancer of any histology and site (including the lung, liver, adrenal, brain, or bone, and other organs) per standard-of-care treatment. Patients under the age of 18 and those unable to provide informed consent were ineligible. No specific eligibility criteria with

regards to concurrent or prior systemic therapy were used. Blood samples were obtained by venipuncture prior to radiation treatment, either at the time of consultation, at simulation, or on the first day of treatment prior to delivery of the first fraction, and 7–14 days after radiation. Approximately 30 ml of blood was collected during each blood draw in10 ml vacutainer blood collection tubes with and without EDTA (for PBMC and serum, respectively) (Becton Dickinson, Franklin Lakes, New Jersey). All blood samples were de-identified before processing of serum and PBMC.

BLOOD PROCESSING AND STORAGE

Whole blood was centrifuged at 1400 rpm for 15 minutes at room temperature. Serum and plasma were aliquoted into cryovials to be frozen at −80°C. Mononuclear cells were isolated via Ficoll-Paque gradient (BD Biosciences). This was centrifuged at 1400 rpm for 5 min at room temp. After RBC lysis, the PBMC were counted for viability and re-suspended in freezing medium (50% IMDM, 40% fetal bovine serum and 10% DMSO) at a concentration of at 1 to 10×10^6 cells/mL. Cells were aliquoted into cryogenic vials and stored at −80°C in the XXXX, where testing was performed by study personnel.

LUMINEX ANALYSIS

Luminex bead-based assays (BioRad, Hercules, CA, USA) were performed on serum specimens from 37 patients to measure circulating levels of 19 cytokines and 11 chemokines (Appendix 1) according to manufacturer's instructions. Most cytokines were assessed using the Cytokine 17-plex assay (M5000031YV), but Cytokine IFN-α2 (171B6010M) was measured using cytokine group II standards (171D6001). TGF-β isoforms 1, 2, and 3 were measured using the TGFβ−1, 2, 3, kit (TGFBNAG-64K-03) (EMD Millpore, Billerica, MA). The majority of the chemokines were measured using the chemokine standard 171DK0001, while RANTES was measured with standard 171B5025M. Concentrations were calculated using a five-parameter standard curve. Serum samples were assayed in duplicate, and averaged to calculate final concentrations.

FLOW CYTOMETRY

PBMC were thawed rapidly in a 37°C water bath and diluted into RF10 media (RPMI 1640 media (ThermoFischer Scientific, USA) with 10% fetal bovine serum and 1% Penicillin/ Streptomycin (Sigma-Aldrich). Cell number and viability were determined using trypan blue exclusion with a hemocytometer after thawing. PBMCs from 30 patients were available for flow cytometry analysis. Immunophenotyping of PBMCs was performed using two panels of antibodies, one panel to characterize NK cells and one to characterize T cells.[37,38] All fluorochrome-conjugated antibodies (Appendix 2) were from BioLegend (San Diego, CA, USA), unless otherwise indicated. Cells were incubated with antibodies diluted in staining buffer (PBS containing 1% human serum and 1% Pen/Strep) at 4°C in the dark for 20 minutes. Cells stained with the NK panel were washed, centrifuged, resuspended in staining buffer, and stored at 4°C. Cells stained with the T cell panel were washed, fixed with Fix/ Perm Buffer (eBiosciences, San Diego, CA, USA) for 30 minutes at 4°C. After washing, cells were resuspended in Perm/Wash buffer containing anti-Foxp3 antibody or isotype control for 30 minutes in the dark at room temperature before being washed and resuspended in staining buffer. Phenotype analysis was done by gating 50,000 to 200,000

cells according to FCS/SSC with a LSR Fortessa flow cytometer using DIVA version6 software (BD Biosciences, San Diego, CA, USA). Data were analyzed using Flow Jo software (Flow Jo LLC, Ashland, OR, USA). Positive and negative cell populations for each marker were determined using fluorescence minus one (FMO) controls[39] and unstained cells were used as a negative control. Instrument settings were verified and adjusted with the mid-peak bead of the 8-peak calibration bead set (Spherotech) before each acquisition session. Compensation beads (BD Biosciences) were used to correct for spectral overlap between channels.

STATISTICAL ANALYSIS

Statistical analyses were carried out using Graph Pad Prism Software (Graph Pad, La Jolla, CA, USA) and R (Vienna, Austria). Baseline characteristics between subgroups were compared using Chi-square tests and one-way analysis of variance (ANOVA). Changes for each parameter across the entire cohort were assessed using paired t-tests. To explore differential response across treatment sites, lung and liver lesions were combined into one cohort called "parenchymal" sites. Differences in immunophenotype changes and cytokine/ chemokine response between parenchymal sites and bone and brain sites were analyzed using one-way analysis of variance (ANOVA) with Bonferroni's post-test for continuous variables to account for multiple comparisons. Chi-square tests were used to identify significant variation across subgroups. Data are presented in bar graphs with vertical bars indicating the mean and lines representing standard error of the mean (SEM). Spearman correlation coefficients were computed for changes in each immune cell population with radiation–associated variables including total dose, dose per fraction and size in cubic centimeters of the planning target volume (PTV). For all tests, statistical significance was assessed at the 0.05 level (2-sided).

RESULTS:

Patient Characteristics

Patients scheduled to undergo SAR to any organ for a primary or metastatic solid tumor prospectively enrolled onto an institutional blood banking protocol between August 2014-June 2017. A total of 40 patients were included in the analysis, 31 enrolled patients had evaluable PBMC samples from pre-SAR and 7–14 days post-SAR, and 37 enrolled patients had pre- and post-treatment serum samples suitable for Luminex analysis of cytokines and chemokines. Of these 40 total patients included in either analysis, 22 (54%) underwent SAR for a lung tumor, 4 (9.8%) underwent SAR to a liver tumor, 9 (22.0%) underwent SAR to a bone lesion, 5 (12.2%) underwent SAR to the brain. One patient (2.4%) was treated to both a lung tumor and soft tissue tumor simultaneously.

Baseline patient characteristics for all patients included in immunophenotyping or Luminex analysis are shown in Table 1. Median age was 68 years (range: 37–86), with 23 men (58%) and 17 women (42%). A non-significant trend toward older median age and greater pack-years smoking history was noted for patients treated to parenchymal sites as compared to brain or bone. Forty-one percent of patients treated to parenchymal sites had received at least one prior course of chemotherapy in their lifetime, as compared to 60–66% of patients

treated to bone or brain (p=0.35). No enrolled patients were receiving systemic dose steroids or concurrent infusional chemotherapy or immunotherapy at the time of SBRT. Seven patients were receiving other cancer-directed systemic therapy at the time of SAR, including androgen deprivation (n=1), endocrine therapy (n=2), tyrosine kinase inhibitor (n=3), and oral capcitabine (n=1). Twenty-four patients had not received cancer-directed systemic therapy within the past year. Among the remaining 9 patients who had received systemic therapy within the past year, the median time from last systemic therapy was 74 days (range: 14–254 days). The median PTV volume was 29.4cc (range, 5.5–118.1) for parenchymal lesions, 48.9cc (11.5–137) for bone lesions and 0.84cc (range, 0.06 –2.08) for brain lesions (p=0.13). The parenchymal group received a median dose of 50 Gy (range, 35–54 Gy) over 3–5 fractions, while the bone group received a median dose of 24 Gy (range, 24–27 Gy) over 3 fractions, and the brain group received a median of 21 Gy (range, 20–21 Gy) in a single fraction (p<0.001). However, the groups were similar in terms of other patient characteristics, as shown in Table 1.

Changes in Natural Killer cells in the Periphery after SAR to Parenchymal Sites

PBMCs from 31 patients were available for flow cytometry analysis. Surface staining of NK cell markers was used in the gating strategy to identify NK cell subsets shown in Figure 1A. There was a statistically significant decrease in the percentage of total NK cells after SAR to parenchymal sites (20.49 +/− 2.36 versus 16.76 +/− 2.436; p=0.01) (Figure 1B and Supplemental Figure 1A). In addition, there was a significant decrease in the percentage of cytotoxic $CD56^{dim}$ $CD16^+$ NK cells after SAR to parenchymal sites (17.58 +/−2.34 versus 13.17+/−2.052; p=0.024) (Figure 1C). No significant change was identified in the percentage of cytokine-producing $CD56^{high}$ $CD16^{neg}$ NK cells in the periphery for any patient cohort. There was no statistically significant change in the percentage of total NK cells, cytotoxic NK cells or cytokine-producing NK cells after SAR to the bone or brain (Figure 1B and Supplemental Figure 1B and 1C). In addition, we identified a statistically significant increase in the percentage of TIM-3+ NK cells in the peripheral blood after SAR to parenchymal sites (15.84+/−3.165 versus 19.65+/−3.261; p = 0.039), but not following SAR to the bone or brain (Figure 2). No statistically significant difference was identified in PD-1 expression on any NK cell subset after SAR (data not shown).

Increase in Activated Memory CD4+ and CD8+ T cells after SAR to Parenchymal sites

Human naïve and memory T cells are distinguished by CD45RA and CD45RO reciprocal isoforms, [40] and central and effector memory T cell subsets are identified based on the expression of CD45R isoforms and either of the homing molecules, CCR7 or CD62L.[41] In this study, we designated CD45RA− CD62L+ T cells to represent central memory T cells (which home to the lymph nodes) and CD45RA− CD62L- cells to represent effector memory T cells which carry out effector functions in the tissue.[41] (Figure 3A) There was a statistically significant increase in the percentage of total CD4+ memory T cells in the PBMC after SAR to parenchymal sites (29.68+/−2.65 versus 38.75+/−3.46; p = 0.026) (Figure 3B and Supplemental Figure 2A), but not after SAR to the bone or brain (Figure 3B and Supplemental Figure 2B and 2C).

Our analysis of the effector and central memory CD4+ T cell compartments focused on the expression of the activation markers, CD25 and ICOS, on memory T cell subsets (Figure 3C and 3D). We identified an increase in the percentage of activated CD4+ memory T cells after SAR as demonstrated by a marked increase in the percentage of ICOS+ CD4+ T cells of total lymphocytes (0.8813+/−0.19 versus 1.739+/−0.241; p = 0.0005) (Figure 3C) and about a two-fold increase in the percentage of activated CD25+ CD4+ T cells after SAR (1.414+/−0.42 versus 2.97+/−0.60; p = 0.078). (Figure 3D). None of these changes were seen after SAR to the bone or brain (Figure 3C and Figure 3D). No change in PD-1 expression was seen in the on the memory CD4+ T cell population after SAR to any site (Supplemental Figure 3). In addition, the percent of CD25+ Foxp3+ CD4+ regulatory T cells did not change after SAR to any site (Supplemental Figure 4).

Analysis of CD8+ memory T cells showed no difference in percent of total CD8+ T cells after SAR (Figure 4A), but did show a strong trend toward an increase in the percentage of activated CD25+ CD8+ memory T cells after SAR to parenchymal sites (1.388+/−0.49 versus 3.50+/−1.10; p = 0.058) (Figure 4B). There were no changes in CD8+ memory T cell populations after SAR to the bone or brain.

Effect of Total Dose, Dose per Fraction, and Planning Target Volume on Immune Cell Populations

Total dose was positively associated with change in % ICOS+ CD4+ memory T cells (Spearman correlation coefficient (r) =0.46, p=0.022) and change in % CD25+ CD8+ memory T cells (r=0.57, p=0.006). The dose per fraction was not associated with any changes in immune cell populations. (Supplemental Table 1). Size of the PTV was positively associated with change in % ICOS+ CD4+ memory T cells (r=0.43, p =0.031) and change in %T regulatory cells (r=0.43, p=0.031). In addition, PTV size was also associated with change in % TIM−3+ NK cells (r=0.48, p=0.008) (Supplemental Table 1).

Changes in Cytokine and Chemokines after SAR to Parenchymal Sites

Serum specimens from 37 patients were evaluable for Luminex analysis. We measured circulating levels of 19 cytokines and 11 chemokines (Appendix 1). Those cytokines and chemokines with >75% of values below the lowest limit of detection (LLOD) were excluded from this analysis. Therefore, the final Luminex analysis included 15 evaluable markers (IL-2, IL-4, IL-6, IL-12, TGF-β1, TGF-β2, TNF-α, IP-10, RANTES, MIP-1α, MIP-1β, MCP-1, MCP-2, and SCYB16). There was a systemic decrease in TNF-α (23.10+/−1.97versus 19.54+/−1.797; p = 0.042), and the chemokines IP-10 (459.4+/−79.76 versus 347.8+/− 44.75; p = 0.048), MCP1 (14.4+/−0.96 versus 11.55+/−1.00; p = 0.0098), MCP2 (172.5+/−18.54 versus 138.6+/−12.43; p = 0.007), MIP-1α (18.67+/−1.49 versus 16.33+/−1.32; p = 0.024), and RANTES (9028+/−864.8 versus 6759+/−485.3; p = 0.035) following SAR to parenchymal sites (Figure 4). Bonferroni correction was used to correct for multiple hypothesis testing. No significant cytokine changes were observed after SAR to the bone or brain (Figure 4). No changes in the pro-inflammatory cytokines IFN-α, IFN-γ or TGF-β were identified.

DISCUSSION:

Due to widespread interest in combining radiation with immunotherapy, there are numerous actively accruing clinical trials are underway that combine SAR with immune checkpoint inhibitors. The scientific rationale for these clinical trials is based on preclinical studies suggesting that radiation can serve as an *in situ* vaccine to augment the effects of immunotherapy, as well as a handful of case reports showing impressive clinical responses to such combinations. However, limited preclinical or clinical data are available to guide the selection of radiation dose, fractionation and site in order to optimally synergize with immunotherapy. We initiated this prospective specimen banking study with a goal of refining our understanding the systemic immune response to SAR monotherapy, and how response differs based on the site irradiated. To our knowledge, no prior studies in patients have directly compared the systemic immune response in patients following SAR to different organs.

There are a few key studies characterizing immune changes following SAR in the setting of concurrent immunotherapy. Tang *et al*. reported that patients who received liver-directed SAR in conjunction with the CTLA-4 inhibitor ipilimumab had enhanced peripheral T-cell activation (GITR+ or LAG3+ CD8+ T-cells) compared with patients that underwent lung-directed SAR.[42] Hiniker *et al* identified an increase in peripheral IL-2-producing CD8+ T-cells and central memory T-cells after radiation in a patient with a complete response to CTLA-4 inhibition and liver-directed SAR.[26] Postow *et al* report detailed immunoprofiling on a patient with progressive melanoma on CTLA-4 blockade who subsequently developed a systemic response following palliative radiotherapy, and noted an increase in ICOS+CD4+T cells, NY-ESO-1 specific IFN-gamma producing CD4+ T cells, and HLA-DR +CD14+monocytes, as well as a decrease in MDSCs.[25]

In addition, there are published reports of the systemic immunophenotype in patients with Stage I or II NSCLC who received SAR alone. Maehata et al described peripheral immune changes that occur following stereotactic body radiotherapy (SBRT) for stage I non-small cell lung cancer (NSCLC), showing that SBRT induces lymphopenia and decreased NK cell activity, which they attribute to radiation directed to vertebral bone marrow in the SBRT field.[28] Trovo et al characterized cytokine changes following SBRT versus conventional radiation for early stage NSCLC, and found a mean reduction of IL-10 and IL-17 plasma levels, but did not look at individual immune cell subsets.[29] Rutkowski et al studied immune cell types after SBRT and observed an increase in the proportion of total CD8+ T cells, total CD4+ T cells, and CD4+ T cells expressing GATA-3, T-bet or ROR-γt, as well as a decrease in CD4+ Foxp3+ regulatory T cells,[43] however this study did not evaluate NK cells. All of these studies examine the immune phenotype after SBRT to the lung alone. To our knowledge, there have been no studies directly comparing the peripheral immune response after SAR to different organs in the absence of concurrent immunotherapy.

We hypothesized that differences in T cell and NK cell activation following radiotherapy to different sites may relate to differences in the degree and potency of immunosuppression of the target tissue. There has been some proof this phenomenon in pre-clinical studies that have shown that intracranial melanoma produces more functional exhaustion and

impairment of T cell effector function than subcutaneous disease with the same tumor histology.[44] To address this question, we focused on the unique tissue microenvironments that characterize the brain, bone, lung, and liver. The brain is characterized by the blood brain barrier (BBB), which sequesters lymphocytes during steady state creating a relatively "immunoprivileged site," but allows lymphocytes to transverse the cerebral vasculature during pathologic states.[45] The bone marrow contains the perivascular hematopoietic stem cell (HSC) niche, which contains mesenchymal stem cells and is characterized by hypoxia, as well as osteoclasts, involved in bone reabsorption, and osteoblasts involved in bone remodeling.[35,46,47,48] In contrast, the lung is in constant contact with toxins and pathogens from the environment during respiration, and bronchial epithelial cells interact with innate immune cells including plasmacytoid dendritic cells, alveolar macrophages, and NK cells, which promote immune tolerance.[49] Similarly, the liver is constantly exposed to antigens transported from the colon via the portal vein, and therefore is composed of an abundance of innate immune cells, such as NK cells, $\gamma\delta$ T cells, and Kupffer cells, which also contribute to immune tolerance.[33] Both the lung and liver develop immune tolerance to the majority of the antigenic load delivered via air exchange or the portal venous blood supply." [33,50] Given the differences in blood supply, antigenic load, and relative abundance of innate immune cells and lymphocytes between these organs, we hypothesized that SAR delivered to these immunotolerant organs would differ from that of immunoprivileged organs such as the brain.

Due to the abundance of NK cells in the lung and liver, we hypothesized that these innate immune cells may play a role in the response to SAR in these organs. While NK cells do not express antigen receptors, they play important roles in viral infections and anti-tumor immunity by cytotoxic killing or the release of IFN-gamma. In humans, two populations of NK cells can be distinguished on the basis of CD56 expression.[51,52] CD56^{dim} cells that express CD16 (the low-affinity receptor for immunoglobulin G, FcRγIII) have enhanced cytotoxicity, while CD56^{hi} NK cells that do not express CD16 (CD56^{hi} CD16$^-$ cells) are able to secrete large amounts of IFN-γ, GM-CSF and TNF-α.[53] Our results show a decrease in both total NK cells and cytotoxic NK cells after SAR to these parenchymal sites. The decrease in NK cells in the peripheral blood after SAR to parenchymal organs could represent increased homing or migration of NK cells to the irradiated tumor site. Previous work in our lab using a patient-derived xenograft model demonstrates decreased tumor volume and increased survival of PDX-bearing mice treated with a combination of radiation and autologous NK cell adoptive therapy.[54] Tumor irradiation in this model leads to tumor cell upregulation of stress ligands such as NKG2D that activate NK cells, and increase homing and infiltration of tagged NK cells into tumor.[54] These findings suggest that the decrease in systemic NK cells after SAR identified in the current study may be secondary to increased NK cell homing to the tumor site. However, we cannot exclude the possibility that the decrease in NK cells seen in the peripheral blood of patients in our study may represent a systemic depletion of NK cells from both the irradiated organs and the peripheral blood.

TIM-3 (T-cell Immunoglobulin- and Mucin-domain-containing molecule-3) was initially identified as a T-helper 1-specific protein involved in regulating T-cell responses, but the highest expression of TIM-3 is found on human NK cells. We saw an increase in circulating TIM-3+ NK cells after SAR to parenchymal sites. Previous studies on TIM-3+ NK cells have focused on their role as exhausted NK cells in several cancers, including melanoma and

colorectal cancer.[55,56] While prior studies have shown that the presence of these cells is associated with worse responses to therapies such as surgery,[56] TIM-3+ NK cells have never been linked to radiation. In aggregate, our data shows that there is a decrease in NK cells in the periphery following SAR but an increase in the TIM-3+ NK cell subset. Future studies will examine the mechanism by which SAR induces NK cell exhaustion and whether anti-TIM-3 antibodies could be used to reverse NK cell exhaustion after radiation.

Given the importance of memory T cells in the induction of the "abscopal" response, we investigated the role of SAR in the induction of memory T cell response. We found an increase in CD4+ memory T cells after SAR to parenchymal sites, with increased expression of ICOS and CD25 activation markers on these cells. Inducible Co-stimulator (ICOS) is a T-cell specific cell surface activation and co-stimulatory molecule structurally related to CD28 and CTLA-4 that increases the proliferation and survival of activated CD4+ effector memory T cells.[42] Anti-CTLA-4 therapy (ipilimumab) increases the frequency of CD4+ T cells expressing ICOS, and these effector T cells produce IFN-gamma.[57] This is due to increased signaling through the phosphinositide-3-kinase (PI3K) pathway and an increase in the expression of T-bet.[58] An increased frequency of ICOS+ CD4+ T cells is associated with improved clinical outcomes for anti-CTLA-4 and anti-OX40 immunotherapies.[57,59] Importantly, this population is not induced by anti-PD-L1 therapy, and may represent a distinct mechanistic pathway of anti-tumor immunity.[60] Our recent clinical data presented here demonstrates that this cell population is also upregulated after SBRT. Therefore, it is possible that activation of ICOS+CD4+ T cells may represent a novel, but synergistic immune mechanism whereby SBRT could enhance PD-L1 checkpoint inhibition.

Unexpectedly, we did not observe any differences in PD-1+ expression on any T cell subsets and did not observe any difference in Foxp3+ regulatory T cells. This could have been because PD-1 is upregulated on antigen-specific T cells, and we were only able to quantify differences in the entire memory T cell population rather than the antigen-specific T cells in our patient samples. However, there are reports in the literature that PD-1, PD-L1, and T regulatory cell markers are decreased after cryopreservation of human PBMC,[61,62] therefore it is possible that our negative finding is due to the limitations of our experimental protocol.

Our Luminex analysis revealed a systemic decrease in TNF-α as well as a decrease in multiple chemokines such as RANTES (CCL5) and IP-10 (CXCL10). RANTES plays a role in homing and migration of effector and memory T cells and helps sustain CD8 T cell responses during a systemic chronic viral infection,[63] therefore it is possible that it is playing a similar role in anti-tumor immunity induced by SAR. IP-10 is IFN-γ-inducible protein 10, and is a chemoattractant for activated memory T cells and NK cells by binding to and activating CXCR3, [64] therefore it may play a role in T cell or NK cell homing after SAR. The systemic decrease in these cytokines is somewhat unexpected given the inflammatory nature of radiotherapy, but has been reported in other studies (Sridharan, 2016). The clinical significance of these decreases and how they relate to changes which may be occurring in the tumor microenvironment is unclear. Future studies are needed to determine if this is due to the reduced half-life, increased degradation, or lower transcription and translation of these cytokines. Unexpectedly, we did not observe changes in the pro-inflammatory cytokines IFN-α, IFN-γ or TGF-β which have been implicated in immune

response to radiation in other studies, perhaps because changes in these cytokines are short-lived. [22, 23, 24, 65]

There are several key limitations to our study, most significantly the inherent baseline differences in radiation dose, fractionation, and target volume size used to treat parenchymal sites vs. bony metastases and brain metastases based on the standard of care treatment for each disease site. It is possible the observed differences in immunophenotype may result from differences in dose and fractionation, rather than treated site. Spearman's correlation coefficients suggest that greater total doses of ablative radiation are associated with an increase in the percentage of activated memory CD4+ and CD8+ T cells. The ablative doses used to irradiate each site are site-dependent, and higher total doses are typically used clinically for liver and lung tumors as compared to brain and bone tumors. Therefore, the observed differences in immune cell populations between sites could be due to the fact that parenchymal lesions are treated to a higher ablative dose than bone and brain lesions. We cannot analyze the contribution of these two variables separately because the study has a limited sample size, and all patients were treated according to the standard of care SAR protocols which allows for minimal variation in dose within each site. An additional limitation is that all of our analyses were performed on batched cryopreserved PBMCs, and there is data to suggest that some biomarkers may be altered in cryopreserved samples.[61,62]

In conclusion, we have identified changes in systemic immunophenotype after SAR to the lung and liver that we do not observe following SAR to the bone and brain. Our findings suggest SAR may be less immunomodulatory when directed to bone or brain, possibly because of the immunosuppressive environment in these organs. We cannot exclude the possibility that differences in the standard-of-care dose schemas for these organs contributed to the observed differences. Correlation between systemic immunophenotype changes and patient outcomes will be crucial to understand the clinical relevance of our finding and the potential for any of these changes to serve as biomarkers. Ultimately, our goal is to use this knowledge about the immune response following SAR to different sites to refine ongoing and future clinical studies combining SAR and immunotherapy.

Supplementary Material

Refer to Web version on PubMed Central for supplementary material.

ACKNOWELDGEMENTS:

REFERENCES:

1. Timmerman R Stereotactic Body Radiation Therapy for Inoperable Early Stage Lung Cancer. JAMA. 2010;303(11):1070. doi:10.1001/jama.2010.261. [PubMed: 20233825]

2. Chi A, Liao Z, Nguyen NP, Xu J, Stea B, Komaki R. Systemic review of the patterns of failure following stereotactic body radiation therapy in early-stage non-small-cell lung cancer: clinical implications. Radiother Oncol. 2010;94(1):1–11. doi:10.1016/j.radonc.2009.12.008. [PubMed: 20074823]

3. Siva S, Slotman BJ. Stereotactic Ablative Body Radiotherapy for Lung Metastases: Where is the Evidence and What are We Doing With It? Semin Radiat Oncol. 2017;27(3):229–239. doi:10.1016/j.semradonc.2017.03.003. [PubMed: 28577830]

4. Su T-S, Liang P, Liang J, et al. Long-Term Survival Analysis of Stereotactic Ablative Radiotherapy Versus Liver Resection for Small Hepatocellular Carcinoma. Int J Radiat Oncol. 2017;98(3):639–646. doi:10.1016/j.ijrobp.2017.02.095.

5. Gkika E, Schultheiss M, Bettinger D, et al. Excellent local control and tolerance profile after stereotactic body radiotherapy of advanced hepatocellular carcinoma. Radiat Oncol. 2017;12(1):116. doi:10.1186/s13014-017-0851-7. [PubMed: 28701219]

6. Chance WW, Nguyen Q-N, Mehran R, et al. Stereotactic ablative radiotherapy for adrenal gland metastases: Factors influencing outcomes, patterns of failure, and dosimetric thresholds for toxicity. Pract Radiat Oncol. 2017;7(3):e195–e203. doi:10.1016/j.prro.2016.09.005. [PubMed: 27743801]

7. Ricardi U, Badellino S, Filippi AR. Clinical applications of stereotactic radiation therapy for oligometastatic cancer patients: a disease-oriented approach. J Radiat Res. 2016;57(S1):i58–i68. doi:10.1093/jrr/rrw006.

8. Formenti SC, Demaria S. Systemic effects of local radiotherapy. Lancet Oncol. 2009;10(7):718–726. doi:10.1016/S1470-2045(09)70082-8. [PubMed: 19573801]

9. Formenti SC, Demaria S. Radiation Therapy to Convert the Tumor Into an In Situ Vaccine. Int J Radiat Oncol. 2012;84(4):879–880. doi:10.1016/j.ijrobp.2012.06.020.

10. Weichselbaum RR, Liang H, Deng L, Fu Y-X. Radiotherapy and immunotherapy: a beneficial liaison? Nat Rev Clin Oncol. 2017;14(6):365–379. doi:10.1038/nrclinonc.2016.211. [PubMed: 28094262]

11. Baird JR, Monjazeb AM, Shah O, et al. Stimulating Innate Immunity to Enhance Radiation Therapy–Induced Tumor Control. Int J Radiat Oncol. 2017;99(2):362–373. doi:10.1016/j.ijrobp.2017.04.014.

12. Young KH, Baird JR, Savage T, et al. Optimizing Timing of Immunotherapy Improves Control of Tumors by Hypofractionated Radiation Therapy. Mattei F, ed. PLoS One. 2016;11(6):e0157164. doi:10.1371/journal.pone.0157164. [PubMed: 27281029]

13. Sharabi AB, Lim M, DeWeese TL, Drake CG. Radiation and checkpoint blockade immunotherapy: radiosensitisation and potential mechanisms of synergy. Lancet Oncol. 2015;16(13):e498–e509. doi:10.1016/S1470-2045(15)00007-8. [PubMed: 26433823]

14. Crittenden M, Kohrt H, Levy R, et al. Current Clinical Trials Testing Combinations of Immunotherapy and Radiation. Semin Radiat Oncol. 2015;25(1):54–64. doi:10.1016/j.semradonc.2014.07.003. [PubMed: 25481267]

15. Formenti SC, Demaria S. Combining Radiotherapy and Cancer Immunotherapy: A Paradigm Shift. *JNCI J Natl Cancer Inst.* 2013;105(4):256–265. doi:10.1093/jnci/djs629. [PubMed: 23291374]

16. Apetoh L, Ghiringhelli F, Tesniere A, et al. Toll-like receptor 4–dependent contribution of the immune system to anticancer chemotherapy and radiotherapy. Nat Med. 2007;13(9):1050–1059. doi:10.1038/nm1622. [PubMed: 17704786]

17. Obeid M, Tesniere A, Ghiringhelli F, et al. Calreticulin exposure dictates the immunogenicity of cancer cell death. Nat Med. 2007;13(1):54–61. doi:10.1038/nm1523. [PubMed: 17187072]

18. Lee Y, Auh SL, Wang Y, et al. Therapeutic effects of ablative radiation on local tumor require CD8+ T cells: changing strategies for cancer treatment. Blood. 2009;114(3):589–595. doi:10.1182/blood-2009-02-206870. [PubMed: 19349616]

19. Klug F, Prakash H, Huber PE, et al. Low-Dose Irradiation Programs Macrophage Differentiation to an iNOS+/M1 Phenotype that Orchestrates Effective T Cell Immunotherapy. Cancer Cell. 2013;24(5):589–602. doi:10.1016/j.ccr.2013.09.014. [PubMed: 24209604]

20. Wu C-Y, Yang L-H, Yang H-Y, et al. Enhanced cancer radiotherapy through immunosuppressive stromal cell destruction in tumors. Clin Cancer Res. 2014;20(3):644–657. doi: 10.1158/1078-0432.CCR-13-1334. [PubMed: 24300786]

21. Crocenzi T, Cottam B, Newell P, et al. A hypofractionated radiation regimen avoids the lymphopenia associated with neoadjuvant chemoradiation therapy of borderline resectable and locally advanced pancreatic adenocarcinoma. J Immunother Cancer. 2016;4(1):45. doi:10.1186/s40425-016-0149-6. [PubMed: 27532020]

22. Vanpouille-Box C, Alard A, Aryankalayil MJ, et al. DNA exonuclease Trex1 regulates radiotherapy-induced tumour immunogenicity. Nat Commun. 2017;8:15618. doi:10.1038/ncomms15618. [PubMed: 28598415]

23. Deng L, Liang H, Xu M, et al. STING-Dependent Cytosolic DNA Sensing Promotes Radiation-Induced Type I Interferon-Dependent Antitumor Immunity in Immunogenic Tumors. Immunity. 2014;41(5):843–852. doi:10.1016/j.immuni.2014.10.019. [PubMed: 25517616]

24. Dewan MZ, Galloway AE, Kawashima N, et al. Fractionated but Not Single-Dose Radiotherapy Induces an Immune-Mediated Abscopal Effect when Combined with Anti-CTLA-4 Antibody. Clin Cancer Res. 2009;15(17):5379–5388. doi:10.1158/1078-0432.CCR-09-0265. [PubMed: 19706802]

25. Postow MA, Callahan MK, Barker CA, et al. Immunologic correlates of the abscopal effect in a patient with melanoma. N Engl J Med. 2012;366(10):925–931. doi:10.1056/NEJMoa1112824. [PubMed: 22397654]

26. Hiniker SM, Chen DS, Reddy S, et al. A systemic complete response of metastatic melanoma to local radiation and immunotherapy. Transl Oncol. 2012;5(6):404–407. http://www.ncbi.nlm.nih.gov/pubmed/23323154. Accessed October 17, 2017. [PubMed: 23323154]

27. Golden EB, Demaria S, Schiff PB, Chachoua A, Formenti SC. An abscopal response to radiation and ipilimumab in a patient with metastatic non-small cell lung cancer. Cancer Immunol Res. 2013;1(6):365–372. doi:10.1158/2326-6066.CIR-13-0115. [PubMed: 24563870]

28. Maehata Y, Onishi H, Kuriyama K, et al. Immune Responses following Stereotactic Body Radiotherapy for Stage I Primary Lung Cancer. Biomed Res Int. 2013;2013:1–11. doi: 10.1155/2013/731346.

29. Trovo M, Giaj-Levra N, Furlan C, et al. Stereotactic body radiation therapy and intensity modulated radiation therapy induce different plasmatic cytokine changes in non-small cell lung cancer patients: a pilot study. Clin Transl Oncol. 2016;18(10):1003–1010. doi:10.1007/s12094015-1473-x. [PubMed: 26687367]

30. Gustafson MP, Bornschlegl S, Park SS, et al. Comprehensive assessment of circulating immune cell populations in response to stereotactic body radiation therapy in patients with liver cancer. Adv Radiat Oncol. 2017;2(4):540–547. doi:10.1016/j.adro.2017.08.003. [PubMed: 29204520]

31. Wild AT, Herman JM, Dholakia AS, et al. Lymphocyte-Sparing Effect of Stereotactic Body Radiation Therapy in Patients With Unresectable Pancreatic Cancer. Int J Radiat Oncol. 2016;94(3):571–579. doi:10.1016/j.ijrobp.2015.11.026.

32. Muraro E, Furlan C, Avanzo M, et al. Local high-dose radiotherapy induces systemic immunomodulating effects of potential therapeutic relevance in oligometastatic breast cancer. Front Immunol. 2017;8:1476. doi:10.3389/fimmu.2017.01476. [PubMed: 29163540]

33. Sun H, Sun C, Tian Z, Xiao W. NK cells in immunotolerant organs. Cell Mol Immunol. 2013;10(3):202–212. doi:10.1038/cmi.2013.9. [PubMed: 23563087]

34. Pardee AD, Butterfield LH. Immunotherapy of hepatocellular carcinoma. Oncoimmunology. 2012;1(1):48–55. doi:10.4161/onci.1.1.18344. [PubMed: 22720211]

35. Méndez-Ferrer S, Michurina TV., Ferraro F, et al. Mesenchymal and haematopoietic stem cells form a unique bone marrow niche. Nature. 2010;466(7308):829–834. doi:10.1038/nature09262. [PubMed: 20703299]

36. Rasid O, Ciulean IS, Fitting C, Doyen N, Cavaillon J-M. Local Microenvironment Controls the Compartmentalization of NK Cell Responses during Systemic Inflammation in Mice. J Immunol. 2016;197(6):2444–2454. doi:10.4049/jimmunol.1601040. [PubMed: 27521338]

37. Lepone LM, Donahue RN, Grenga I, et al. Analyses of 123 Peripheral Human Immune Cell Subsets: Defining Differences with Age and between Healthy Donors and Cancer Patients Not Detected in Analysis of Standard Immune Cell Types. J Circ Biomarkers. 2016;5:5. doi: 10.5772/62322.

38. Donahue RN, Lepone LM, Grenga I, et al. Analyses of the peripheral immunome following multiple administrations of avelumab, a human IgG1 anti-PD-L1 monoclonal antibody. J Immunother Cancer. 2017;5(1):20. doi:10.1186/s40425-017-0220-y. [PubMed: 28239472]

39. Baumgarth N, Roederer M. A practical approach to multicolor flow cytometry for immunophenotyping. J Immunol Methods. 2000;243(1–2):77–97. http://www.ncbi.nlm.nih.gov/pubmed/10986408. Accessed August 8, 2017. [PubMed: 10986408]

40. Michie CA, McLean A, Alcock C, Beverley PCL. Lifespan of human lymphocyte subsets defined by CD45 isoforms. Nature. 1992;360(6401):264–265. doi:10.1038/360264a0. [PubMed: 1436108]

41. Sallusto F, Lenig D, Förster R, Lipp M, Lanzavecchia A. Two subsets of memory T lymphocytes with distinct homing potentials and effector functions. Nature. 1999;401(6754):708–712. doi: 10.1038/44385. [PubMed: 10537110]

42. Tang C, Welsh JW, de Groot P, et al. Ipilimumab with Stereotactic Ablative Radiation Therapy: Phase I Results and Immunologic Correlates from Peripheral T Cells. Clin Cancer Res. 2017;23(6):1388–1396. doi:10.1158/1078-0432.CCR-16-1432. [PubMed: 27649551]

43. Rutkowski J, lebioda T, Kmie Z, Zaucha R. Changes of systemic immune response after stereotactic ablative radiotherapy (SABR) - first results of a prospective study in early lung cancer patients. Polish Arch Intern Med. 2017;127(4):245–253. doi:10.20452/pamw.3997.

44. Jackson CM, Kochel CM, Nirschl CJ, et al. Systemic Tolerance Mediated by Melanoma Brain Tumors Is Reversible by Radiotherapy and Vaccination. Clin Cancer Res. 2016;22(5):1161–1172. doi:10.1158/1078-0432.CCR-15-1516. [PubMed: 26490306]

45. Louveau A, Harris TH, Kipnis J. Revisiting the Mechanisms of CNS Immune Privilege. Trends Immunol. 2015;36(10):569–577. doi:10.1016/j.it.2015.08.006. [PubMed: 26431936]

46. Bussard KM, Gay CV., Mastro AM. The bone microenvironment in metastasis; what is special about bone? Cancer Metastasis Rev. 2008;27(1):41–55. doi:10.1007/s10555-007-9109-4. [PubMed: 18071636]

47. Takubo K, Goda N, Yamada W, et al. Regulation of the HIF-1α Level Is Essential for Hematopoietic Stem Cells. Cell Stem Cell. 2010;7(3):391–402. doi:10.1016/j.stem.2010.06.020. [PubMed: 20804974]

48. Morrison SJ, Scadden DT. The bone marrow niche for haematopoietic stem cells. Nature. 2014;505(7483):327–334. doi:10.1038/nature12984. [PubMed: 24429631]

49. Bals R, Hiemstra PS. Innate immunity in the lung: how epithelial cells fight against respiratory pathogens. Eur Respir J. 2004;23(2):327–333. http://www.ncbi.nlm.nih.gov/pubmed/14979512. Accessed September 17, 2017. [PubMed: 14979512]

50. Lau AH, Thomson AW. Dendritic cells and immune regulation in the liver. Gut. 2003;52(2):307–314. http://www.ncbi.nlm.nih.gov/pubmed/12524419. Accessed May 22, 2017. [PubMed: 12524419]

51. Di Santo JP. Natural killer cells: diversity in search of a niche. Nat Immunol. 2008;9(5):473–475. doi:10.1038/ni.f.201. [PubMed: 18425102]

52. Lanier LL, Le AM, Civin CI, Loken MR, Phillips JH. The relationship of CD16 (Leu-11) and Leu-19 (NKH-1) antigen expression on human peripheral blood NK cells and cytotoxic T lymphocytes. J Immunol. 1986;136(12):4480–4486. http://www.ncbi.nlm.nih.gov/pubmed/3086432. Accessed August 19, 2017. [PubMed: 3086432]

53. Cooper MA, Fehniger TA, Caligiuri MA. The biology of human natural killer-cell subsets. Trends Immunol. 2001;22(11):633–640. http://www.ncbi.nlm.nih.gov/pubmed/11698225. Accessed August 19, 2017. [PubMed: 11698225]

54. Ames E, Canter RJ, Grossenbacher SK, et al. Enhanced targeting of stem-like solid tumor cells with radiation and natural killer cells. Oncoimmunology. 2015;4(9):e1036212. doi: 10.1080/2162402X.2015.1036212. [PubMed: 26405602]

55. da Silva IP, Gallois A, Jimenez-Baranda S, et al. Reversal of NK-Cell Exhaustion in Advanced Melanoma by Tim-3 Blockade. Cancer Immunol Res. 2014;2(5):410–422. doi: 10.1158/23266066.CIR-13-0171. [PubMed: 24795354]

56. Wang Y, Sun J, Gao W, et al. Preoperative Tim−3 expression on peripheral NK cells is correlated with pathologic TNM staging in colorectal cancer. Mol Med Rep. 2017;15(6):3810–3818. doi: 10.3892/mmr.2017.6482. [PubMed: 28440449]

57. Ng Tang D, Shen Y, Sun J, et al. Increased Frequency of ICOS+ CD4 T Cells as a Pharmacodynamic Biomarker for Anti-CTLA-4 Therapy. Cancer Immunol Res. 2013;1(4):229–234. doi:10.1158/2326-6066.CIR-13-0020. [PubMed: 24777852]

58. Chen H, Fu T, Suh W-K, et al. CD4 T Cells Require ICOS-Mediated PI3K Signaling to Increase T-Bet Expression in the Setting of Anti-CTLA-4 Therapy. Cancer Immunol Res. 2014;2(2):167176. doi:10.1158/2326-6066.CIR-13-0155.

59. Metzger TC, Long H, Potluri S, et al. ICOS Promotes the Function of CD4+ Effector T Cells during Anti-OX40-Mediated Tumor Rejection. Cancer Res. 2016;76(13):3684–3689. doi: 10.1158/0008-5472.CAN-15-3412. [PubMed: 27197182]

60. Wei SC, Levine JH, Cogdill AP, et al. Distinct Cellular Mechanisms Underlie Anti-CTLA-4 and Anti-PD-1 Checkpoint Blockade. Cell. 2017;170(6):1120–1133.e17. doi:10.1016/j.cell. 2017.07.024. [PubMed: 28803728]

61. Sattui S, de la Flor C, Sanchez C, et al. Cryopreservation modulates the detection of regulatory T cell markers. Cytom Part B Clin Cytom. 2012;82B(1):54–58. doi:10.1002/cyto.b.20621.

62. Campbell DE, Tustin NB, Riedel E, et al. Cryopreservation Decreases Receptor PD-1 and Ligand PD-L1 Coinhibitory Expression on Peripheral Blood Mononuclear Cell-Derived T Cells and Monocytes. Clin Vaccine Immunol. 2009;16(11):1648–1653. doi:10.1128/CVI.00259-09. [PubMed: 19726615]

63. Crawford A, Angelosanto JM, Nadwodny KL, Blackburn SD, Wherry EJ. A role for the chemokine RANTES in regulating CD8 T cell responses during chronic viral infection. Douek DC, ed. PLoS Pathog. 2011;7(7):e1002098. doi:10.1371/journal.ppat.1002098. [PubMed: 21814510]

64. Dufour JH, Dziejman M, Liu MT, Leung JH, Lane TE, Luster AD. IFN-gamma-inducible protein 10 (IP-10; CXCL10)-deficient mice reveal a role for IP-10 in effector T cell generation and trafficking. J Immunol. 2002;168(7):3195–3204. http://www.ncbi.nlm.nih.gov/pubmed/11907072. Accessed August 19, 2017. [PubMed: 11907072]

65. Vanpouille-Box C, Diamond JM, Pilones KA, et al. TGF Is a Master Regulator of Radiation Therapy-Induced Antitumor Immunity. Cancer Res. 2015;75(11):2232–2242. doi: 10.1158/00085472.CAN-14-3511. [PubMed: 25858148]
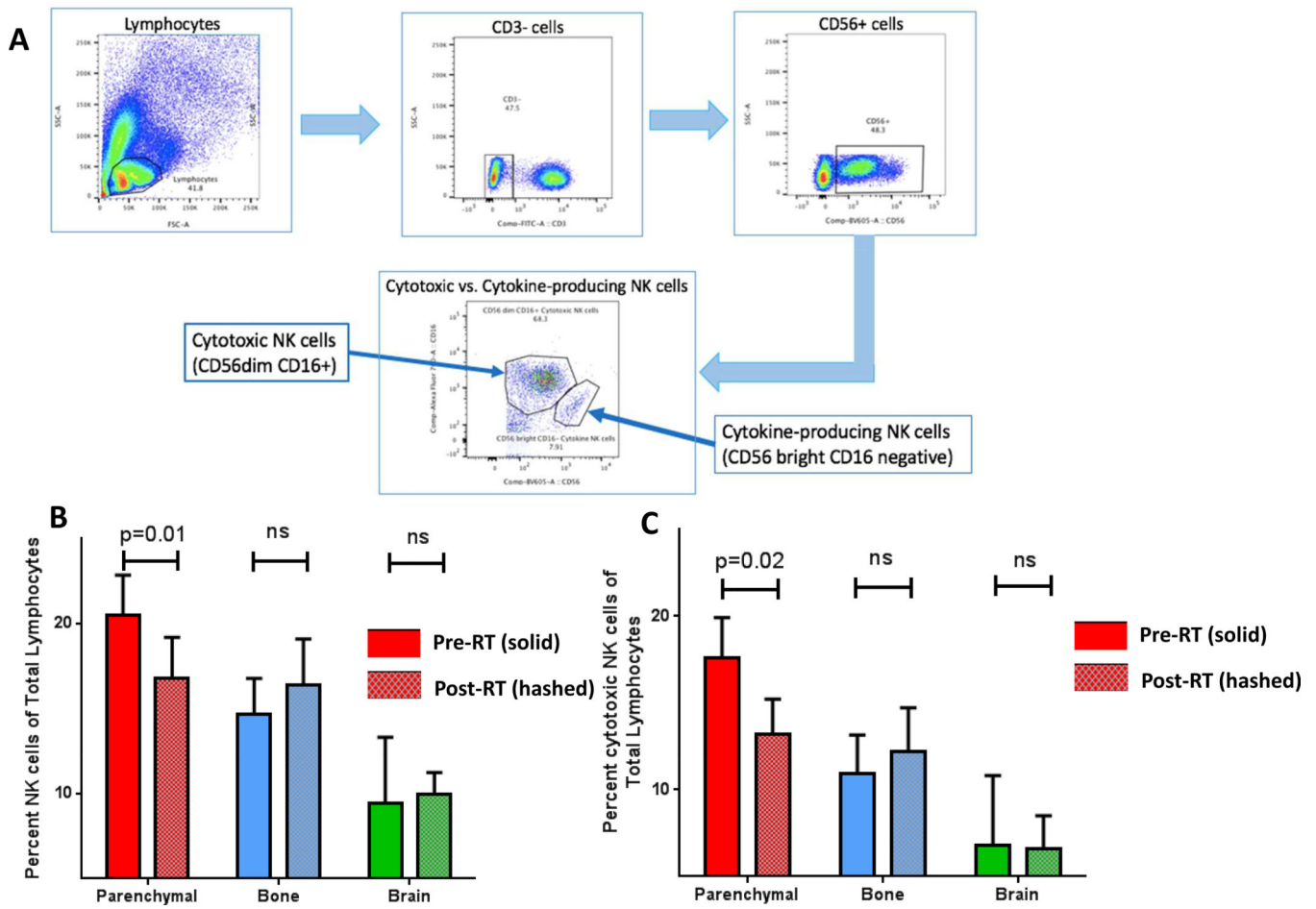
Figure 1: Decrease in the total and cytotoxic NK cells after SAR to parenchymal Sites, but not bone or brain.
A. Gating strategy for identification of Natural Killer cell subsets from total lymphocytes in PBMC. **B.** **T**otal NK cells in PBMC after SAR to parenchymal sites, bone and brain. **C.** Cytotoxic NK cells in PBMC after SAR to parenchymal sites, bone and brain.
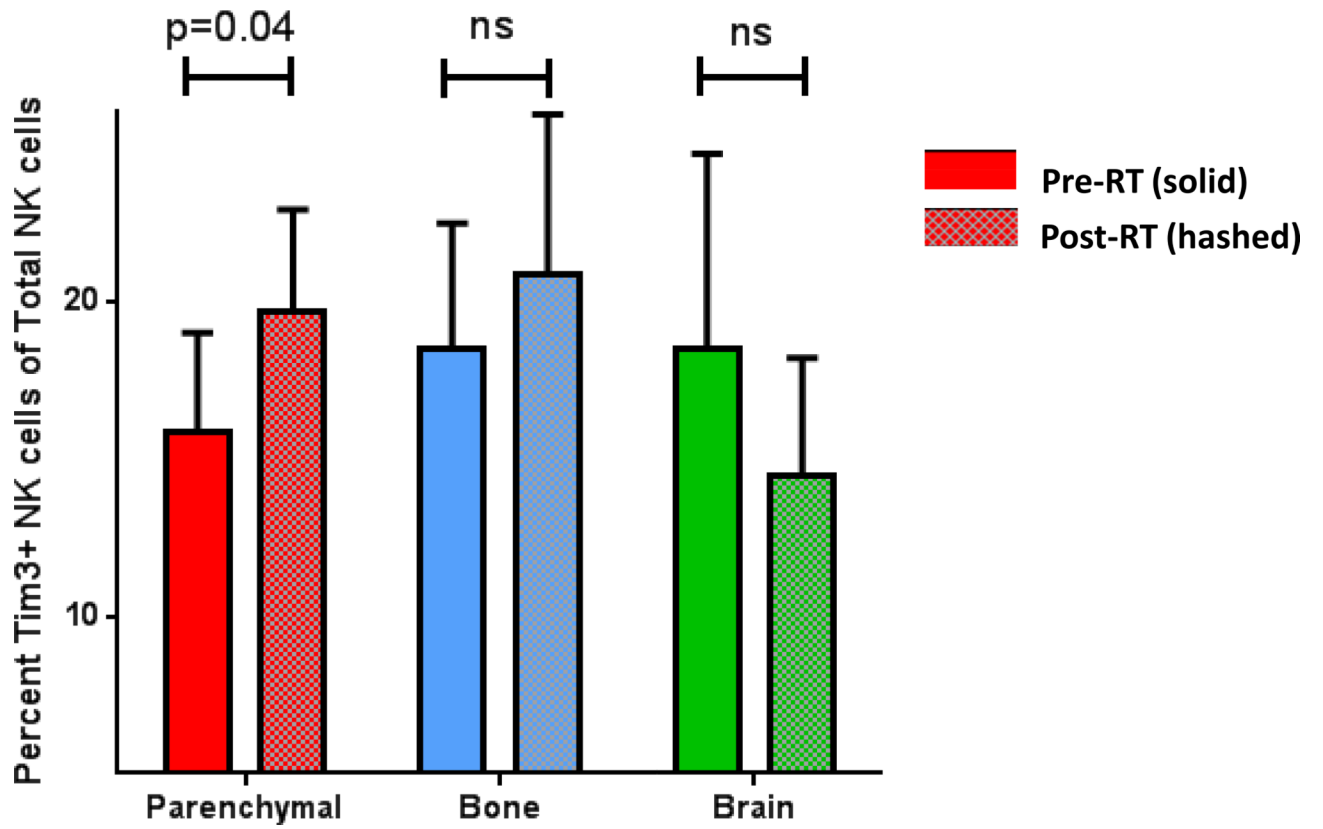
Figure 2: Increase in TIM3+ NK cells after SAR to parenchymal sites.
Percent TIM3+ NK cells of the total NK cell population in PBMC after SAR to parenchymal sites (red), bone (blue), and brain (green).
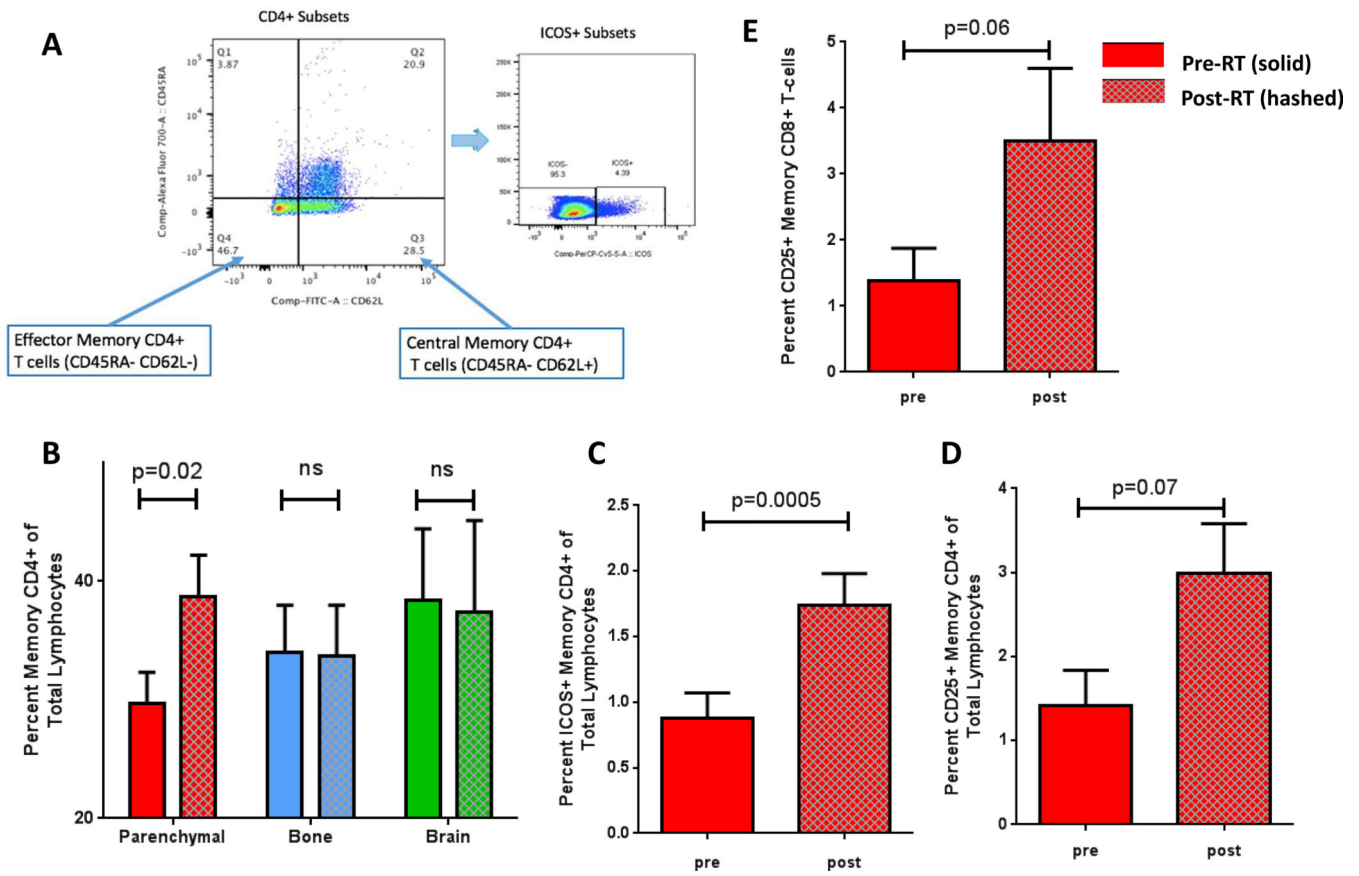
Figure 3: SAR causes increases in memory CD4+ and CD8+ T cell populations, including activated ICOS+ and CD25+ memory T cells.

A. Gating strategy for memory CD4+ T cell subsets and activated ICOS+ cells. **B.** Memory CD4+ T cell populations after SAR to parenchymal organs, bone, and brain. **C.** Activated ICOS+ CD4+ memory T cell population after SAR to parenchymal sites alone. **D.** Activated CD25+ Memory CD4+ T cell populations after SAR to parenchymal sites alone. **E.** Activated CD25+ memory CD8+ T cells after SAR to parenchymal sites alone.
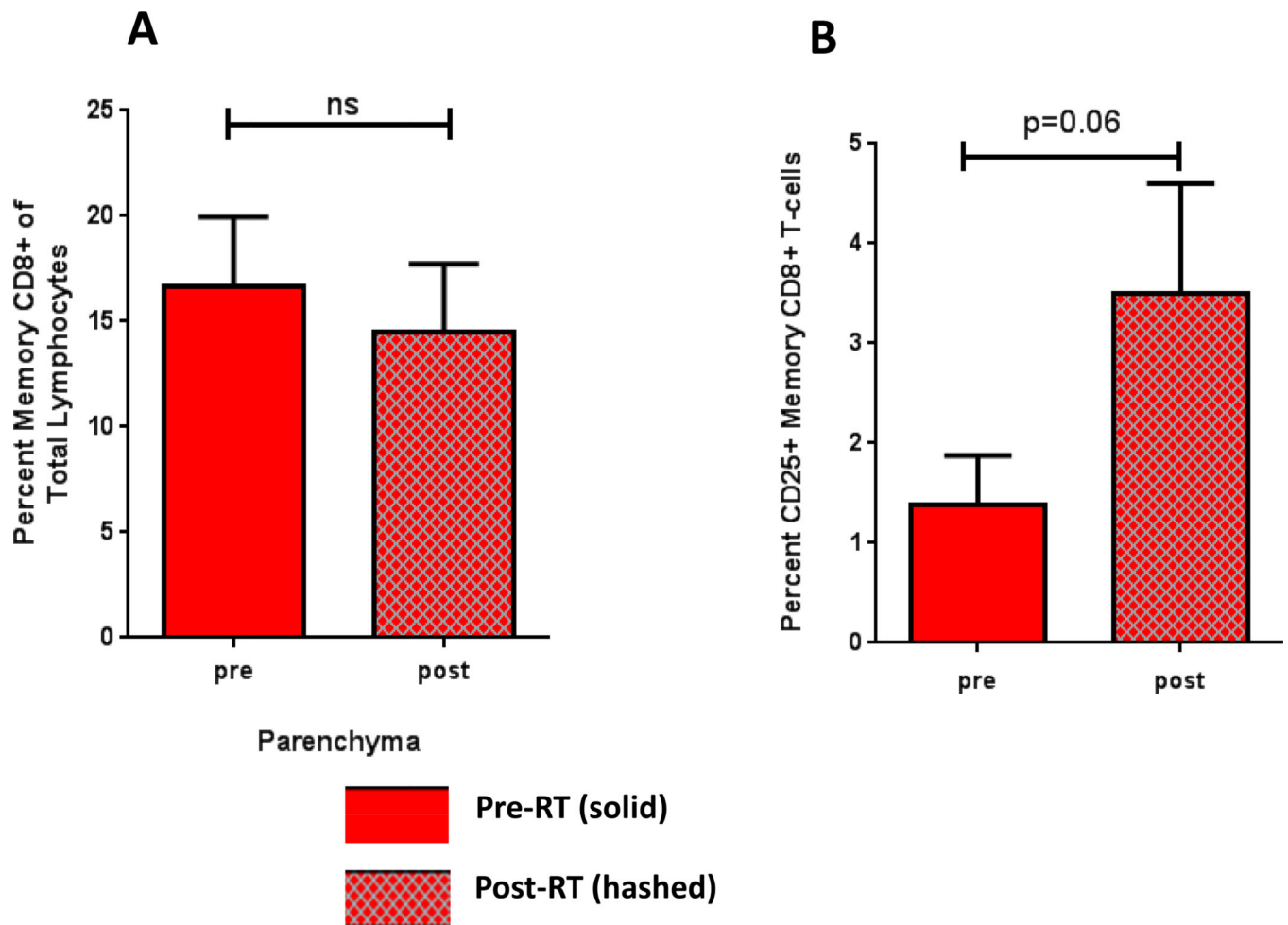
Figure 4: SAR causes an increase in the activated CD25+ memory CD8+ T cells.
A. Percent CD8+ memory T cells after SAR to parenchymal sites. **B**. Percent activated CD25+ memory CD8+ T cells after SAR to parenchymal sites.
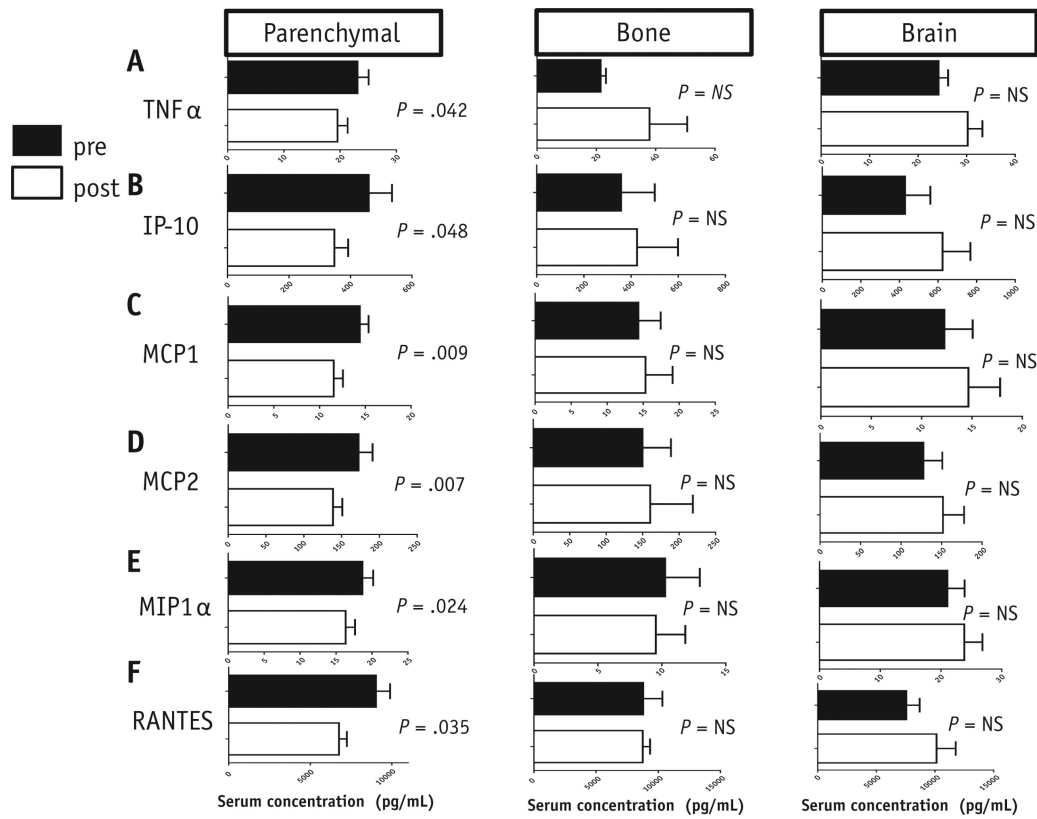
Figure 5:
Luminex analysis of cytokines and chemokines in the serum of patients treated with SAR to parenchymal, bone, and brain sites. **A.** TNF-alpha. **B.** IL-10. **C.** MCP-1. **D.** MCP-2. **E.** MIP-1 alpha. **F.** RANTES. (All cytokine and chemokine concentrations are in pg/mL)

Table 1:

Patient Characteristics

	Parenchymal (lung and liver) n=26	Bone (n=9)	Brain (n=5)	p-value
Age Median (range)	71 (30–86)	64 (37–78)	66 (48–74)	0.13
PTV (cc) Median (range)	31.3 (5.5–277.8)	48.9 (11.5–174.1)	0.8 (0.6–2.1)	0.13
Disease Stage				
I	20	0	0	
II	1	0	0	
IV	5	9	5	
Pack-year smoking Median (range)	13 (0–120)	0 (0–30)	15 (0–40)	0.17
Dose (Gy) Median (range)	50 (35–54)	24 (24–27)	21 (20–21)	**<0.00001**
Number of fractions Median (range)	5 (3–5)	3 (3–3)	1 (1–1)	**<0.00001**
Histology (%)				0.46
Adenocarcinoma	12 (46%)	7 (78%)	2 (40%)	
Squamous	5 (19%)	0	1 (20%)	
Sarcoma	3 (12%)	0	0	
Undifferentiated/ other	3 (12%)	2 22%)	2 (40%)	
Unbiopsied	3 (12%)	0	0	
Prior systemic therapy (% Yes)	38%	78%	60%	0.11
Cytoxic chemotherapy	8	0	2	
Endocrine therapy	0	3	1	
Immunotherapy	0	1	1	
Targeted Therapy	2	3	0	

Abbreviations: PTV = Planning Tumor Volume, Pack-years = number of pack-years of smoking cigarettes in the patient's lifetime, Endocrine therapy = endocrine therapies for metastatic prostate cancer